ilmedia

TECHNISCHE UNIVERSITÄT
ILMENAU

Niemeyer, Markus; Kleinschmidt, Peter; Walker, Alexandre W.; Mundt, Laura Elena; Timm, Cornelia; Lang, Robin; Hannappel, Thomas; Lackner, David:

Measurement of the non-radiative minority recombination lifetime and the effective radiative recombination coefficient in GaAs

Original published in:	AIP Advances / American Institute of PhysicsNew York, NY : American Inst. of Physics. - 9 (2019), 4, art. 045034, 7 pp.
Original published:	2019-04-30
ISSN:	2158-3226
DOI:	10.1063/1.5051709
[*Visited:*	2020-02-11]

This work is licensed under a Creative Commons Attribution 4.0 International license. To view a copy of this license, visit http://creativecommons.org/licenses/BY/4.0/

TU Ilmenau | Universitätsbibliothek | ilmedia, 2020
http://www.tu-ilmenau.de/ilmedia

Measurement of the non-radiative minority recombination lifetime and the effective radiative recombination coefficient in GaAs

Cite as: AIP Advances 9, 045034 (2019); doi: 10.1063/1.5051709
Submitted: 11 August 2018 • Accepted: 8 April 2019 •
Published Online: 30 April 2019

View Online

Export Citation

CrossMark

M. Niemeyer,[1,a] P. Kleinschmidt,[2] A. W. Walker,[3] L. E. Mundt,[1] C. Timm,[2] R. Lang,[1] T. Hannappel,[2] and D. Lackner[1]

AFFILIATIONS

[1] Fraunhofer Institute for Solar Energy Systems, ISE, Heidenhofstraße 2, 79110 Freiburg, Germany
[2] Technische Universität Ilmenau, Institut für Physik, 98693 Ilmenau, Germany
[3] National Research Council of Canada, 1200 Montreal Road, M-50, Ottawa, Ontario K1A 0R6, Canada

[a] Author to whom correspondence should be addressed: markus.niemeyer@ise.fraunhofer.de

ABSTRACT

The combination of time-resolved (TR) and power-dependent relative (PDR) photoluminescence (PL) measurements reveals the possibility of separating the radiative and non-radiative minority carrier lifetimes and measuring the sample-dependent effective radiative recombination coefficient in direct bandgap semiconductors. To demonstrate the method, measurements on 2 µm thick p-type GaAs double-hetero structures were conducted for various doping concentrations in the range of $5x10^{16}$ and $1x10^{18}$ cm^{-3}. With a photon recycling factor of 0.76 ± 0.04 the radiative recombination coefficient was determined to be $(3.3\pm0.6)\times10^{-10}$ cm^3s^{-1} for the structures with a doping concentration below $1*10^{18}$ cm^{-3}, whereas the effective radiative recombination parameter for an absorber thickness of 2 µm was directly measured to be $(0.78\pm0.07)\times10^{-10}$ cm^3s^{-1}. For a doping concentration of 1×10^{18} cm^{-3}, the radiative recombination coefficient decreases significantly probably due to the degeneracy of the semiconductor.

© 2019 Author(s). All article content, except where otherwise noted, is licensed under a Creative Commons Attribution (CC BY) license (http://creativecommons.org/licenses/by/4.0/). https://doi.org/10.1063/1.5051709

I. INTRODUCTION

It has recently been shown that photon recycling must be considered for the modelling of highly-efficient optoelectronic devices.[1–3] Photon recycling within the active layer is effectively increasing the minority carrier lifetime associated with the radiative recombination process τ_{rad}^{eff}.[4] This is often taken into account by introducing a photon-recycling factor f.[4] Other authors[5] have included this factor in defining an effective radiative recombination coefficient as shown in equation (1), where N denotes the activated dopant density and Δn denotes the excess carrier density in this context.

$$\frac{1}{\tau_{rad}^{eff}} = \frac{(1-f)}{\tau_{rad}} = (1-f)B_{rad}(N+\Delta n) = B_{rad}^{eff}(N+\Delta n) \qquad (1)$$

where B_{rad}^{eff} depends primarily on the radiative recombination parameter of the active material, but also depends strongly on the geometry of the sample, especially the thickness of the active layer and the presence of any mirrors on the rear-side (after substrate removal).[6] It is possible to calculate both the photon recycling factor and B_{rad}^{eff}.[1,5] However, these calculations are strongly dependent on accurate knowledge of the sample geometry and absorption data close to the bandgap. As ternary and quaternary alloys are becoming more adopted, such absorption data may not be known to sufficient accuracy. Thus, a direct measurement approach is of great interest.

Furthermore, from an experimental material development point of view, the quality of optoelectronic semiconductor material is often rated in terms of the minority carrier recombination lifetime. This lifetime is a combination of several recombination channels: radiative and non-radiative recombination, such as Shockley-Read-Hall (SRH) recombination[7–10] including interface recombination via traps, and finally Auger recombination. While radiative recombination, i.e. the spontaneous emission of photons, is unavoidable,

non-radiative recombination can be reduced by advanced preparation, thus creating a material with a low defect density. For this optimization, a direct measurement of the lifetime associated with the non-radiative recombination channel is very helpful. There are other methods to disentangle these two recombination mechanisms, such as fitting of nonlinear high-injection time-resolved photoluminescence (TR-PL) measurements,[11] analyzing the temperature dependence of TR-PL[12] or both.[13] In order to extract the low-injection bulk-lifetime via monoexponential decay, sufficiently high initial carrier-density must be established in order to achieve quasi-equilibrium with metastable trap states,[11] and the carrier density must also be sufficiently low to not enter the non-monoexponential high-injection regime.

There are several methods to determine the radiative efficiency at low injection.[14,15,12] Recently, a simple photoluminescence (PL) method was reported based on power-dependent relative PL (PDR-PL) which measures the effective radiative efficiency from low to high injection.[5] However, all steady-state measurement methods for radiative efficiency face the challenge of calibration as they are not absolute. This is solved by the assumption of pure radiative recombination at high injection[5] or low temperature,[14] which is only valid for certain samples.

The PDR-PL measurement routine as described has two limitations: firstly, it is necessary to calculate the photon recycling factor from known material properties (i.e. absorption and emission, see for example Refs. 1 and 5) and secondly, purely radiative recombination has to be achieved for self-calibration. For the latter Auger and defect recombination have to be negligible compared to radiative recombination at high injection, which may or may not be the case depending on the material and its quality. Furthermore, band filling of the indirect bands as well as carrier escape out of the double-heterostructure (DH) via thermionic emission must both be negligible; fortunately for the AlGaAs/GaAs material system, the barrier height is sufficient.[16] In other words, these constraints are not necessarily given for every sample investigated. Thus, two components are required to further validate the PDR-PL method: first a direct method of extracting B_{rad}^{eff} and second, a calibration of the PDR-PL signal. For this purpose, TR-PL can be used to quantify the effective radiative efficiency under low injection conditions when combined with the knowledge of the effective radiative recombination coefficient B_{rad}^{eff}. The result is a calibrated low-injection radiative efficiency used to calibrate the PDR-PL signal, which serves to quantify the high injection radiative efficiency of the system.

In the approach suggested, it is possible to determine the sample-dependent B_{rad}^{eff} of a DH, and its excess carrier density dependent effective radiative efficiency. However, the Auger coefficient of the material must be known, and the TR-PL lifetime has to be limited by defect recombination, i.e. not trap filling. In the case of known photon recycling properties (i.e. absorption and emission), the material-specific B_{rad} can be extracted.

As an example, measurements are performed on p-GaAs DHs with different doping concentrations in the test layer. These samples are described in section II, as well as the measurement methods of TR-PL and PDR-PL. In section III, the calculation of B_{rad}^{eff} is given, followed by the calibration of the PDR-PL measurement in section IV. As both calculations depend on each other, as a last step, the calculations are performed iteratively. Results from the investigated samples are discussed and the benefits of combining PDR-PL with TR-PL are demonstrated. Finally, the results are summarized in section VI.

II. EXPERIMENTAL DETAILS

A. Sample description

Four $Al_{0.70}Ga_{0.30}As/GaAs/Al_{0.70}Ga_{0.30}As$ DH were grown in an AIX2800-G4-TM metal organic vapor phase (MOVPE) reactor with a p-doping concentration of 5×10^{16} cm^{-3}, 1×10^{17} cm^{-3}, 2.5×10^{17} cm^{-3}, and 1×10^{18} cm^{-3} in the test layer, respectively. The layer stack used for each sample is shown in Figure 1. Nine periods of strain-compensated quantum wells were included to remove any luminescence coupling between the substrate and the test structure. No increase of threading dislocation density was observed by plain view cathodoluminescence measurements due to the quantum wells. The four samples were deposited on semi-insulating GaAs substrates at a growth temperature of 590 °C and a V/III ratio of 32.

The doping concentrations of the test layers were measured by electrochemical capacitance-voltage; a measurement uncertainty of 10% was assumed for the doping concentration. The effective lifetime was determined by TR-PL and the unscaled effective radiative efficiency by PDR-PL.[5] Both photoluminescence measurement setups are described below.

B. Experimental setups

1. Time-resolved photoluminescence

The effective minority carrier lifetime was measured by TR-PL. The DHs were excited by a pulsed laser light employing a 640 nm diode laser (PicoQuant). The decay of the radiative band-to-band recombination was measured by a single photon counting avalanche photodiode (id Quantique) combined with a time-correlated single photon counting unit (PicoHarp 300). The excess carrier density per pulse (cm^{-3}) was calculated by the laser spot size, the test layer thickness, the surface reflection, the repetition rate of the laser and the cw laser power, which was measured by a calibrated photodiode at the position of the sample. The overall time resolution given by the width of the system response function was 150 ps. The effective lifetime was extracted from the measured photoluminescence signal by fitting a single exponential decay function.

	Layer	Function	Thickness	Doping
	i-GaAs	cap	10 nm	---
	p-$Al_{0.75}Ga_{0.25}As$	barrier	100 nm	4*10^{17} cm^{-3}
	p-GaAs	test layer	2000 nm	N_A
	p-$Al_{0.75}Ga_{0.25}As$	barrier	100 nm	4*10^{17} cm^{-3}
9x	i-$Ga_{0.60}In_{0.40}P$	QW-barrier	25 nm	---
9x	i-$Ga_{0.85}In_{0.15}As$	QW-barrier	33 nm	---
9x	i-$Ga_{0.60}In_{0.40}P$	QW-barrier	25 nm	---
	i-GaAs	substrate	450 µm	---

FIG. 1. Sketch of the double-hetero structures deposited on semi-insulating GaAs wafers. The strain balanced quantum well (QW) structures suppress luminescence coupling between the substrate and the test layer. Doping concentration (N_A) was varied between the different samples.

© Author(s) 2019

In order to extract the true bulk recombination lifetime from TR-PL measurements, it is essential that the lifetime does not change with excess carrier density when fitting the decay of the PL signal by a monoexponential decay function; otherwise, carrier trapping effects are impacting the signal as a function of excess carrier density. In the samples discussed, the bulk minority lifetime is extracted for low excess carrier densities Δn, where Δn is negligible compared to the doping density N. Additionally, TR-PL is not a steady state measurement. Therefore carriers trapped by shallow metastable states can have a strong impact on the TR-PL signal.[11,13,17] The mono-exponential behavior of the PL decay combined with our estimated initial carrier density suggest that the excess carrier density is significant compared to the shallow metastable trap states; this is confirmed by the agreement between the extracted and calculated values of B_{rad}^{eff}. This renders the decay lifetime as approximately representative of the effective bulk lifetime.

2. Power-dependent relative photoluminescence

The PDR-PL measurement setup and routine are described in detail elsewhere[5] and will therefore only be summarized concisely. The sample was illuminated by a 532 nm 0.5 W laser in cw operation. The resulting wavelength-resolved PL signal of the test layer was measured by a charged coupled device (Andor Technology, DU401A-BR-DD). The laser intensity on the sample was decreased stepwise over seven orders of magnitude by a neutral density filter wheel and the resulting PL signal was measured for each step. The PL signal of each intensity step was integrated over the photoluminescence peak and divided by the laser power to get the integrated so-called relative PL intensity. The relative PL signal was normalized to the maximum relative PL signal which is now defined as I_{rel}. If there is a stable plateau at the maximum of I_{rel}, recombination can be assumed to be purely radiative at this plateau, and the measured normalized relative PL signal is equal to the effective radiative efficiency η_{eff}. However, 100% radiative recombination cannot be reached in every sample.

III. MEASUREMENT RESULTS

A. Effective lifetime at low injection measured by TR-PL

The decay of the photoluminescence signal was measured by TR-PL for different laser intensities, which are equivalent to different excess carrier densities Δn. The normalized TR-PL measurement signal for the lowest laser intensity of each sample is shown in Figure 2. The signals measured at low injection are all monoexponential, whereas the analysis of non-monoexponential decays would need special attention.[11,13,17] At these low excitation densities, the monoexponential time constant is assumed to be equivalent to the effective bulk minority carrier lifetime; this assumption will be tested later when comparing the extracted effective radiative recombination coefficient to that calculated from theory.

The resulting time constants from the monoexponential fits depicted in Figure 2 show an increase in effective lifetime with increasing doping concentration. Note that these lifetimes are significantly shorter than the expected radiative lifetimes assuming the often quoted value of B_{rad} for GaAs of 10^{-10} cm^3/s.[6,18,19] This indicates that nonradiative recombination is critical in these samples

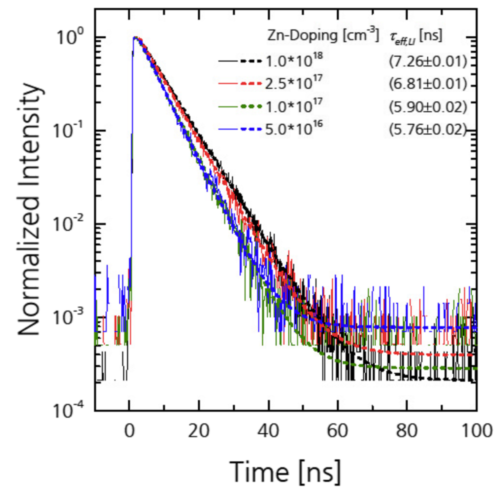

FIG. 2. Normalized time-resolved photoluminescence decay measurements (solid lines) and fits (dashed) for the lowest laser pulse energy applied. The initial carrier density for these measurements is in the range of $10^{13}-10^{14} cm^{-3}$, as shown in Figure 3.

for low injection, which can explain the increase in effective lifetime with increasing doping concentration.

The extracted monoexponential time constants from TR-PL measurements with varying laser pulse intensity are shown in Figure 3 as a function of excess carrier concentration. The lifetime is constant when $\Delta n \ll N$ is fulfilled. The monoexponential time constants at low injection are therefore equivalent to the effective bulk minority carrier lifetime at these excitation densities.

B. PDR-PL

The relative photoluminescence signal I_{rel} normalized to 1 and measured by PDR-PL is shown in Figure 4. For all samples a constant I_{rel} was measured at low laser power, concluding that the samples

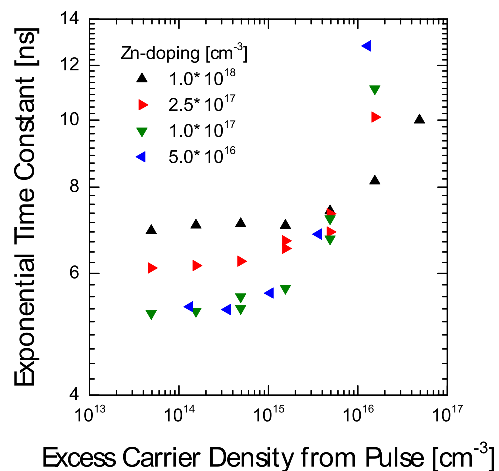

FIG. 3. Extracted monoexponential time constants from TR-PL measurements for increasing laser pulse intensities, equivalent to increasing excess carrier densities.

© Author(s) 2019

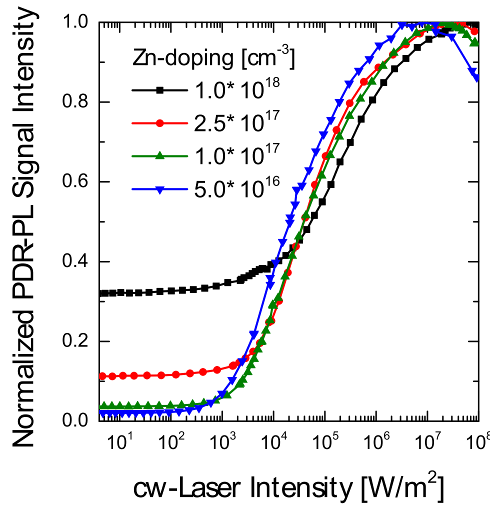

FIG. 4. Normalized relative photoluminescence signal I_{rel} of four AlGaAs/GaAs DHs with different p-doping concentration measured by PDR-PL. For all samples, I_{rel} is constant at low laser intensities. A measurement uncertainty of 10% was assumed for all measurement points.

were probed in low injection conditions and a constant effective lifetime is given in this regime. Additionally signals from all samples reach a plateau at high laser power before they drop again at the highest laser power. Further analysis is not possible at this point as each PDR-PL signal has to be scaled individually. Furthermore laser power and excess carrier density are linked by the lifetime which depends strongly on doping concentration, which varies between samples. Therefore jumping to conclusions based purely on the PDR-PL measurements can be misleading.

IV. CALCULATION OF THE EFFECTIVE RADIATIVE RECOMBINATION COEFFICIENT

As mentioned, the defect lifetime of minority carriers is a crucial measure of semiconductor material quality. However, TR-PL measures the effective lifetime τ_{eff} which depends on the effective radiative τ_{rad}^{eff} (i.e. the spontaneous emission lifetime weighted by the probability of photon escape out of the DH) and non-radiative τ_{NR} lifetime as given by:

$$\frac{1}{\tau_{eff}} = \frac{1}{\tau_{rad}^{eff}} + \frac{1}{\tau_{NR}} = \frac{1}{\tau_{rad}^{eff}} + \frac{1}{\tau_{aug}} + \frac{1}{\tau_{srh}}. \tag{2}$$

Typically τ_{NR} is linked to Auger recombination (τ_{Aug}) and defect recombination (τ_{SRH}) including interface recombination. The effective radiative efficiency η_{eff} is the probability of radiative recombination which results in emission out of the front surface of the DH, and can be expressed as:

$$\eta_{eff} = \frac{\tau_{eff}}{\tau_{rad}^{eff}}. \tag{3}$$

Knowing τ_{eff} and η_{eff} of a sample thus allows for the separation of the radiative and non-radiative components to the effective lifetime.

Therefore, equations (2) and (3) can be combined, resulting in the effective radiative lifetime

$$\tau_{rad}^{eff} = \frac{1}{\eta_{eff}} \tau_{eff}, \tag{4}$$

and the non-radiative lifetime

$$\tau_{NR} = \frac{1}{1 - \eta_{eff}} \tau_{eff}. \tag{5}$$

A calculation of the effective radiative recombination coefficient B_{rad}^{eff} for a given structure is possible as τ_{rad}^{eff} can be approximated by

$$\frac{1}{\tau_{rad}^{eff}} \cong B_{rad}^{eff}(N + \Delta n), \tag{6}$$

if N is orders of magnitude higher than the intrinsic free carrier concentration, which is impacted by the doping concentration in degenerate semiconductors,[20] but is in the range of 10^6 cm^{-3} for GaAs at room temperature.[21]

Combining equations (4) and (6) reveals the possibility to calculate B_{rad}^{eff}. Note that B_{rad}^{eff} depends on the absorption and emission properties of the material, as well as its thickness since this strongly impacts photon recycling in contrast to the Einstein coefficient B_{rad}. It can be shown that B_{rad}^{eff} can be calculated as follows:

$$B_{rad}^{eff} \cong \frac{\eta_{eff,LI}}{\tau_{eff,LI} N_{A,D}}, \tag{7}$$

where B_{rad}^{eff} depends on the low injection effective radiative efficiency $\eta_{eff,LI}$. If an effective radiative recombination of 1 is reached within the measurement, η_{eff} is equivalent to the normalized PDR-PL signal. Otherwise a calibration of the PDR-PL signal is necessary, which is discussed in the next section.

V. CALIBRATION OF THE PDR-PL SIGNAL

We will now take a look closer look at steady state conditions, under which PDR-PL measurements are performed. At steady state, the generation rate G is balanced with the recombination rate U via the continuity equation:

$$\frac{\partial \Delta n}{\partial t} = G - U = 0, \tag{8}$$

where Δn is the excess carrier concentration in the test layer (with thickness d and associated relative absorption A) depending on illumination with a cw laser (photon energy E_{ph}, intensity I_{laser}), which is therefore defined by

$$\Delta n = \tau_{eff}\, G = \tau_{eff} \frac{I_{laser} A}{E_{ph} d}, \tag{9}$$

where the effective lifetime (defined by equation (2)) is related to defect recombination τ_{srh}, radiative recombination (equation (1)), and Auger recombination $\tau_{aug} = (C_{aug}(N + \Delta n)^2)^{-1}$, where C_{aug} is the Auger recombination coefficient. The Auger lifetime can be calculated if the Auger recombination coefficient C_{aug} is known, as it is for GaAs: $C_{aug} = (7 \pm 4) * 10^{-30}$.[22]

Therefore the effective radiative efficiency η_{eff} can be calculated using equations (2) and (3):

© Author(s) 2019

$$\frac{1}{\eta_{eff}} = \tau_{rad}^{eff}\left(\frac{1}{\tau_{aug}} + \frac{1}{\tau_{rad}^{eff}} + \frac{1}{\tau_{srh}}\right), \tag{10}$$

assuming a known τ_{srh}.

Vice versa: for a known η_{eff} the excess carrier density dependent τ_{srh} can be calculated and fitted for m different types of defects by the minority (τ_{min}) and majority carrier defect lifetimes (τ_{maj}) of each defect type:[7]

$$\frac{1}{\tau_{srh}} = \sum_i^m \frac{1}{\tau_{srh,i}} = \sum_i^m \frac{1}{\tau_{min,i} + y\ \tau_{maj,i}}; y = \frac{\Delta n}{N + \Delta n}. \tag{11}$$

Note that τ_{srh} is dominated by the defect type with the shortest lifetime, which could be surface recombination. It is possible that the defect type dominating the SRH lifetime changes with Δn.

The measured PDR-PL signal represents the effective radiative efficiency only if a radiative efficiency of unity is reached in the measurement. In this case, the measurement is self-calibrated. Most samples, however, do not reach complete effective radiative efficiency due to material quality, or a low bandgap (which results in significant Auger recombination) for example, and a calibration of the PDR-PL measurement is necessary. This calibration is done using a known B_{rad}^{eff} and a calculation of the excess carrier density dependent τ_{eff}. The calibration factor x_{rad} for the PDR-PL signal is defined as:

$$\eta_{eff} = x_{rad}\ I_{rel}. \tag{12}$$

x_{rad} can be calculated iteratively with the excess carrier density dependent lifetimes for Auger, radiative and defect recombination (fit from equation (11) to measured data) at the maximum of the PDR-PL signal:

$$x_{rad} = \frac{\tau_{eff}(\Delta n(I_{rel,max}))}{\tau_{rad}(\Delta n(I_{rel,max}))} \tag{13}$$

The process is iterative and converges for all samples investigated. A fit of the SRH-lifetime with $m = 2$ defect types to the data obtained for the sample with $N = 2.5 \times 10^{17}\ cm^{-3}$ is shown in Figure 5.

VI. RESULTS AND DISCUSSION

Calculating B_{rad}^{eff} and x_{rad} is an iterative process since both depend on each other; in other words, a decreased radiative efficiency η_{eff} leads to a corrected B_{rad}^{eff} (see equation (7)) which itself leads to a corrected η_{eff}. For all samples investigated, the iterative process converges independently of the starting parameters for τ_{eff} and x_{rad}.

The excess carrier density dependent SRH lifetimes (equation (6)) are calculated and shown in Figure 7. The SRH lifetimes of all samples saturate within the low injection regime and increase with excess carrier density. At the highest radiative efficiency the measured lifetime does not reach a plateau, highlighting the inadequate assumption of a purely radiative system, and afterwards subsequently drops for most samples. This could be attributed to a number of factors, including measurement uncertainty at high injection, the uncertainty of the Auger coefficient of GaAs, and lastly, carrier spilling over the barriers via thermionic emission. In contrast to low injection, the SRH lifetime of the samples decreases at high injection for increasing doping concentration.

Using the measurement results shown in Figure 3 and Figure 4, the radiative efficiencies η_{eff} were calculated for the four samples and are shown in Figure 6 together with the calculated radiative efficiency, assuming two types of defects are limiting the SRH lifetime.

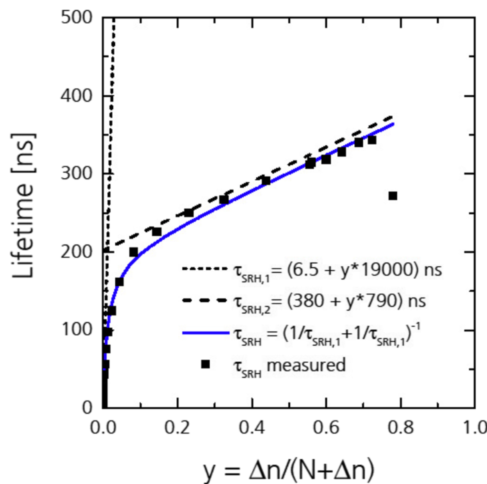

FIG. 5. Extracted SRH lifetime (squares) dependent on injection level y, as defined in equation (11) for the GaAs-DH with a doping concentration of $2.5 \times 10^{17}\ cm^{-3}$. Fitted SRH lifetime with two defect types (type one: black, type two: red, resulting: blue solid line), as defined in equation (11), which results in a minority carrier and majority carrier lifetime for both defects.

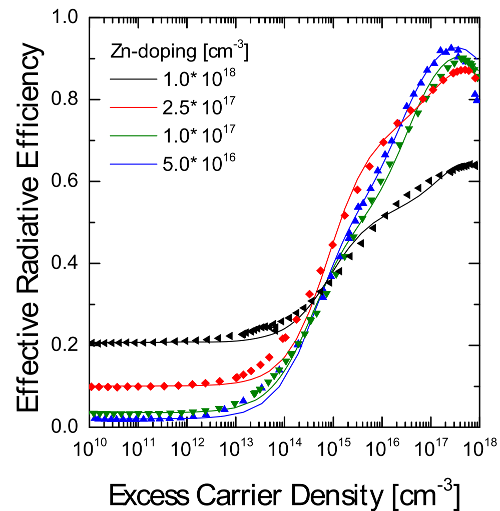

FIG. 6. Excess carrier dependent radiative efficiencies of the four samples investigated. Symbols are the measured lifetimes; lines are the calculated lifetimes with a SRH lifetime for two defect types. A measurement uncertainty of 10% from the PDR-PL measurement and an uncertainty of 5% from the fit was assumed for all measurement points.

© Author(s) 2019

Comparing the onset of the increase in τ_{eff} measured by TR-PL (Figure 3) and τ_{SRH} measured by PDR-PL (Figure 7) reveals a difference in excess carrier density of this point with a factor of about one order of magnitude. One reason for that is the change in excess carrier density of several orders of magnitude over one TR-PL measurement. A monoexponential fit is not adequate in the case of a non-constant lifetime. A second reason is that both measurement methods suffer from the fact that the excess carrier density is assumed constant in the probing area. Since the laser beam cross section is not a rectangular function but rather Gaussian in nature, this assumption can lead to uncertainties in the calculated excess carrier density in both measurement methods.

Lifetimes at low injection are shown in Figure 8 for all samples. The non-radiative lifetime includes defect recombination in the bulk as well as at the interfaces. A separation of both is possible by a thickness variation of the test layer. As shown in previous measurements,[5] the defect lifetime of the samples investigated is dominated by bulk recombination. The measured non-radiative lifetimes are comparable to some published data (2 μm thick p-type sample: 1.0×10^{18} cm^{-3}, τ_{eff}: 8.5 ns[4,23]) but orders of magnitude smaller than others reported for samples showing a biexponential decay (2 μm thick p-type sample: 2.4×10^{17} cm^{-3}, τ_{eff}: 350 ns[17]). The low growth temperature of 590 °C could be a reason for this limited lifetime.[24] Usually the opposite behavior is expected as the dopant itself, or impurities in the dopant source, may decrease the material quality with increasing concentration. Here, a decline of the recombination rate with doping is observed. This behavior can be explained by the uncertainty of the measurement, but a similar behavior has been reported for the EL2 defect in n-GaAs samples.[25] Calculations suggest that the formation energy of a Ga antisite or a Ga vacancy is increased with p-doping concentration for As-rich growth,[26] which would hint at these defects limiting the samples defect lifetime. Deep-level transient spectroscopy conducted on specially designed samples could clarify this behavior.

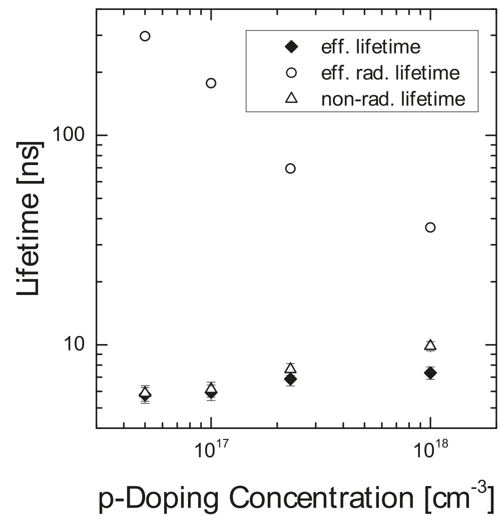

FIG. 8. Measured effective lifetime as well as effective radiative and non-radiative lifetimes of p-GaAs for different Zn-doping concentrations at low injection conditions.

Even though the SRH lifetime at low injection increases with doping concentration, the trends are completely reversed for increasing injection. This example shows that a measure of the lifetime at low injection is not sufficient for device optimization, as the operation point of minority carrier devices, such as concentrator solar cells operating under up to 2000 times concentrated solar radiation, is mostly at higher carrier densities.

Furthermore, the effective radiative recombination coefficient B_{rad}^{eff} of the DH-structures were deduced from equation (7) and are shown in Figure 9. For the same samples the effective radiative

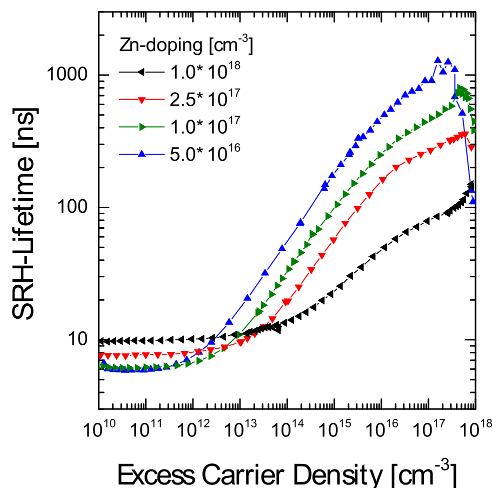

FIG. 7. Deduced excess carrier dependent SRH lifetimes for the four samples investigated. Calculated from PDR-PL measurements, calibrated by TR-PL measurements.

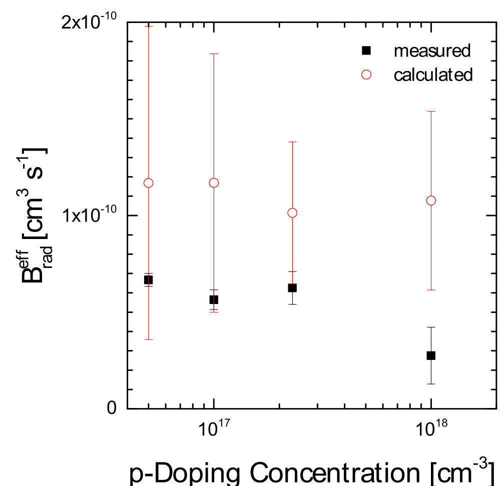

FIG. 9. Effective radiative recombination coefficient B_{rad}^{eff} for 2 μm thick GaAs double-hetero structures. Error bars for the measured values are from the uncertainty of C_{aug} = $(7 \pm 4) cm^6 s^{-1}$,[22] the laser power density (±50%), doping concentration (±10%), and TR-PL low injection lifetime as noted in Figure 2.

© Author(s) 2019

recombination coefficients were also calculated in a similar fashion to Lumb *et al.*[1] using doping dependent refractive indices of GaAs[18] to compute the relative absorption within and outside the critical angle of emission inside the DH for a particular thickness of 2 μm. Note that the model assumes that the photon recycling factor is not a function of bias (or light intensity), which is a limitation of this model; accounting for the dependence of bias or excess carrier density results in significant complications in the calculations. The bandgap is extracted optically from measured PL spectra at room temperature to account for bandgap narrowing effects.[27] The results of these calculations are also shown in Figure 9.

The agreement between the extracted values of the B_{rad}^{eff} and the calculated B_{rad}^{eff} are rather poor. However, large uncertainties of the calculated values of B_{rad}^{eff} arise from the impact of doping concentration on the intrinsic carrier concentration, which has been shown to be significant.[28,29] Unfortunately, this impact is not clearly visible analyzing the TR-PL lifetimes of p-GaAs double-heterostructures as a function of doping, as done in by Steiner et al.,[6] since the range of doping concentration was not fully explored and there is significant scatter in the data. In fact, there is subtle evidence that the radiative lifetime is increasing beyond the expected trend for a constant value of B_{rad}. This highlights the need for more thorough experimental validation of the impact of high carrier concentrations on both radiative recombination as well as the radiative lifetime.

The B_{rad} of GaAs was then calculated using equation (1), since the photon recycling factor in GaAs was previously determined to be 0.74[5] or 0.80[1] for 2 μm GaAs absorber structures. For the low-doped samples, a radiative recombination coefficient B_{rad} of $(3.3\pm0.6)\times10^{-10}$ cm^3/s was measured. This is around a factor of two lower than the value calculated by Varshni in 1976,[30] but in agreement with values calculated by Casey *et al.*[19] For a doping concentration of 10^{18} cm^{-3}, B_{rad} decreases to $(2.1\pm0.4)\times10^{-10}$ cm^3/s. For highly doped samples ($N > 1\times10^{18}$ cm^{-3}), a decrease of B_{rad} is expected due to the degenerate state of the semiconductor, leading to a decrease of the slope of the absorption coefficient close to the bandgap. A similar effect was also measured for n-doped GaAs.[31]

VII. CONCLUSION

The combination of time-resolved photoluminescence and power-dependent relative photoluminescence reveals a method to determine the radiative and non-radiative lifetimes of a double heterostructure. Furthermore, the combination of those two measurement methods enables the measurement of the radiative efficiency and the effective radiative recombination coefficient.

It was shown that the low injection non-radiative lifetime of the investigated MOVPE grown Zn-doped GaAs samples increased with doping concentration for the growth conditions chosen. The radiative recombination coefficient for bulk GaAs was determined to be $(3.3\pm0.6)\times10^{-10}$ cm^{3}s^{-1} for the structure with a doping concentration below $1*10^{18}$ cm^{-3}, whereas the effective radiative recombination parameter for the sample with an absorber thickness of 2 μm was directly measured to be $(0.78\pm0.07)\times10^{-10}$ cm^{3}s^{-1}. For a doping concentration of 1×10^{18} cm^{-3}, the radiative recombination coefficient decreases significantly probably due to the degeneracy of the semiconductor.

ACKNOWLEDGMENTS

This work was partly funded by the German BMWi through the project HekMod4 (contract 0325750) and MatProzell (contract 50RN1501). The authors would like to thank Dr. Klaus Schwarzburg for discussions about TR-PL and J. Schön for those about excess carrier dependent defect lifetimes. Further the technical support on the MOVPE reactors by S. Stättner, and K. Wagner is greatly appreciated. M. Niemeyer acknowledges the scholarship support from the German Federal Environmental Foundation (DBU).

REFERENCES

[1] M. P. Lumb, M. Steiner, J. F. Geisz, and R. J. Walters, J. Appl. Phys. **116**, 194504-1–194504-10 (2014).
[2] A. W. Walker, O. Hohn, D. N. Micha, B. Bläsi, A. W. Bett, and F. Dimroth, IEEE J. Photovolt. **5**, 1636 (2015).
[3] J. F. Geisz, M. Steiner, I. Garcia, S. R. Kurtz, and D. J. Friedman, Appl. Phys. Lett. **103**, 041118 (2013).
[4] P. Asbeck, J. Appl. Phys. **48**, 820 (1977).
[5] A. W. Walker, S. Heckelmann, C. Karcher, O. Höhn, C. Went, M. Niemeyer, A. W. Bett, and D. Lackner, J. Appl. Phys. **119**, 155702 (2016).
[6] M. Steiner, J. F. Geisz, I. Garcia, D. J. Friedman, A. Duda, W. J. Olavarria, M. Young, D. Kuciauskas, and S. R. Kurtz, IEEE J. Photovolt. **3**, 1437 (2013).
[7] W. Shockley and W. T. Read, Phys. Rev. **87**, 835 (1952).
[8] R. N. Hall, Phys. Rev. **87**, 387 (1952).
[9] R. N. Hall, Proceedings of the IEE - Part B: Electronic and Communication Engineering **106**, 923 (1959).
[10] V. K. Khanna, Progress in Quantum Electronics **29**, 59 (2005).
[11] M. W. Gerber and R. N. Kleiman, Journal of Applied Physics **122**, 095705 (2017).
[12] M. W. Gerber and R. N. Kleiman, Journal of Applied Physics **121**, 225702 (2017).
[13] M. Maiberg, T. Hölscher, S. Zahedi-Azad, and R. Scheer, Journal of Applied Physics **118**, 105701 (2015).
[14] T. H. Gfroerer, L. P. Priestley, M. F. Fairley, and M. W. Wanlass, J. Appl. Phys. **94**, 1738 (2003).
[15] S. Komiya, A. Yamaguchi, and I. Umebu, Solid-State Electronics **29**, 235 (1986).
[16] E. E. Perl, D. Kuciauskas, J. Simon, D. J. Friedman, and M. Steiner, Journal of Applied Physics **122**, 233102 (2017).
[17] R. K. Ahrenkiel, N. Call, S. W. Johnston, and W. K. Metzger, Solar Energy Materials and Solar Cells **94**, 2197 (2010).
[18] M. Levinshtein, S. Rumyantsev, and M. Shur, eds., *Si, Ge, C (Diamond), GaAs, GaP, GaSb, InAs, InP, InSb* (World Scientific Publishing, Singapore, 1996).
[19] H. C. Casey, Jr. and F. Stern, J. Appl. Phys. **47**, 631 (1976).
[20] H. S. Bennett and J. R. Lowney, Journal of Applied Physics **62**, 521 (1987).
[21] J. S. Blakemore, Journal of Applied Physics **53**, 520 (1982).
[22] U. Strauß, W. W. Rühle, and K. Köhler, Appl. Phys. Lett. **62**, 55 (1993).
[23] M. Ettenberg and H. Kressel, J. Appl. Phys. **47**, 1538 (1976).
[24] H. Ito, T. Furuta, and T. Ishibashi, Appl. Phys. Lett. **58**, 2936 (1991).
[25] J. Lagowski, H. C. Gatos, J. M. Parsey, K. Wada, M. Kaminska, and W. Walukiewicz, Appl. Phys. Lett. **40**, 342 (1982).
[26] H.-P. Komsa and A. Pasquarello, Journal of Physics. Condensed Matter: An Institute of Physics Journal **24**, 045801 (2012).
[27] P. van Mieghem, R. P. Mertens, G. Borghs, and R. J. van Overstraeten, Phys. Rev. B **41**, 5952 (1990).
[28] H. S. Bennett, Journal of Applied Physics **60**, 2866 (1986).
[29] H. S. Bennett, J. Appl. Phys. **83**, 3102 (1998).
[30] Y. P. Varshni, Physica Status Solidi (B) **20**, 9 (1967).
[31] G. B. Lush, Sol. Energy Mater. Sol. Cells **93**, 1225 (2009).

© Author(s) 2019